Structure, phase transition and impedance of $Zn_{1-x}Li_xO$ ($0.10 \leq x \leq 0.70$) ceramic

U. Ahmadu & Islamiyat Temitope Salaudeen

Applied Physics A
Materials Science & Processing

ISSN 0947-8396
Volume 122
Number 7

Appl. Phys. A (2016) 122:1-10
DOI 10.1007/s00339-016-0213-6

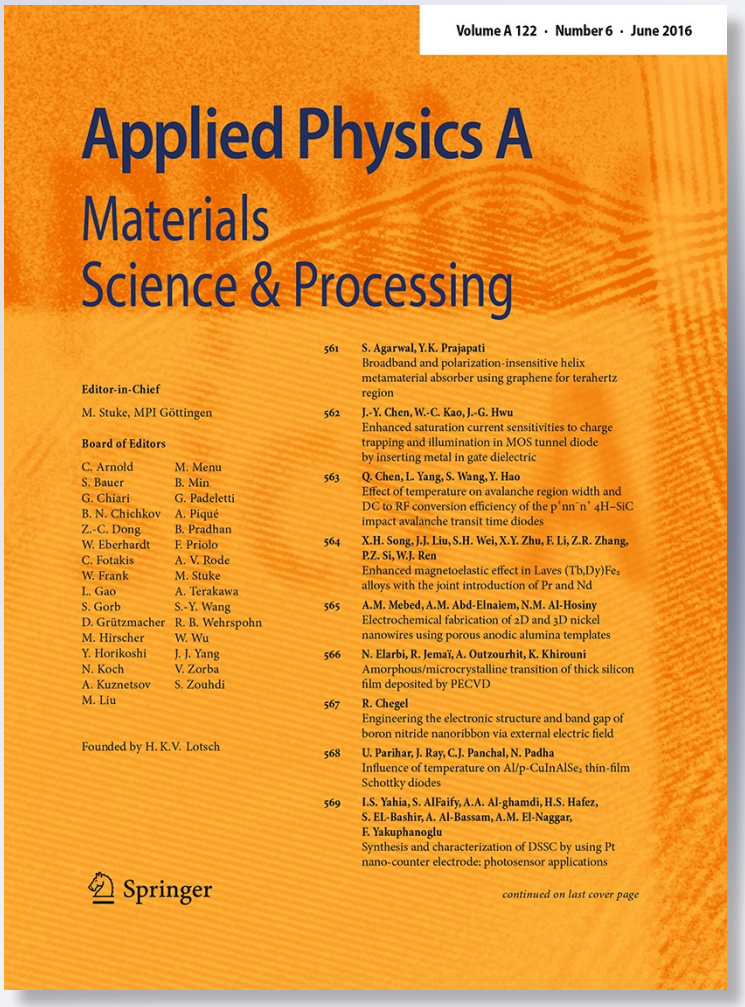

Springer

Appl. Phys. A (2016)122:693
DOI 10.1007/s00339-016-0213-6

Applied Physics A
Materials Science & Processing

Structure, phase transition and impedance of $Zn_{1-x}Li_xO$ ($0.10 \leq x \leq 0.70$) ceramic

U. Ahmadu[1] · Islamiyat Temitope Salaudeen[1]

Received: 11 April 2016 / Accepted: 12 June 2016

Abstract Structural transformations of Li-doped $Zn_{1-x}Li_xO$ ($0.10 \leq x \leq 0.70$) which was synthesised by solid-state reaction were investigated. XRD carried out on powder specimens of the samples show that they are polycrystalline in nature with a hexagonal wurtzite structure having minor impurities. The result indicates the maximum limit of substitution of Zn atoms by Li is at $x = 0.4$. The lattice parameter a reduced from 3.01 to 2.99 Å, while c reduced from 5.21 to 5.19 Å. However, the Zn–O bond length reduced from 1.88 to 1.87 Å for the undoped, to $x = 0.60$ for the doped, respectively. The c/a ratio is 1.73 and is almost constant for all samples. The grain size of the (100) peak of the undoped ZnO is 41.73 nm and that of $x = 0.10$ is 41.76 nm. For $x = 0.2$–0.70, the grain size is 41.72 nm indicating that the grain size is almost independent of doping. The SEM results indicate a variation of grain size from 2.18 to 5.15 μm for the undoped ZnO to $x = 0.50$, which shows increase in grain size and reduction in grain boundaries as doping increases. The results show that $x = 0.50$ has the highest grain size and the one with the highest transition temperature is $x = 0.6$. DTA results indicate the structural phase transition temperature of the doped ZnO ranged from ~371 to ~409 K and increased as the amount of Li increases. A single arc is observed in all the impedance plots of the ZnO together with the presence of a relaxation process which is non-Debye. The impedance data show reduced resistance with increase in lithium content. A general increase in dielectric constant with increase in lithium content is observed.

✉ U. Ahmadu
u.ahmadu@yahoo.com

[1] Department of Physics, Federal University of Technology, Minna, Nigeria

1 Introduction

There has been renewed interest in research on ZnO films as transparent conducting coating materials due to their low cost and resistivity, high transparency in the visible region and high light trapping properties [1]. It exhibits properties such as piezoelectricity, strong photoluminescence, high electron mobility, thermal conductivity and a wide and direct band gap [2, 3].

ZnO is an intrinsic semiconductor with band gap of 3.2 eV at room temperature and crystallises in the hexagonal wurtzite lattice with space group Pb_3mc [1, 4]. It is generally n-type due to native defects created during its preparation which have been attributed to excess zinc in the interstitial position or oxygen vacancy or both [1]. Doping ions larger in size than Zn ions substitute Zn sites and may result in the dopants being inserted between Zn and oxygen ions because of the small size of the ion [5]. ZnO has been doped with several dopants including Li. Discrepancies in results have been obtained on several of its physical properties when different dopants are used and even when in its pristine form. These have been reported on dielectric anomaly, ferroelectric transition and phase transition temperatures, to mention but a few. Theoretical calculations show that group I elements are better dopants than those of group V in terms of acceptor levels where energies could be up to 0.09 eV in the case of Li-substituting Zn, which is the shallowest level amongst energy levels of acceptor dopants reported [2]. On the other hand, experimentally, 30 % of the Zn sites have been found to be occupied by Li in single crystals of ZnO, but the substitution is easily followed by the formation of interstitial Li which are most likely to be shallow donors causing p-type doping to be limited by the formation of interstitial Li complex.

Published online: 23 June 2016

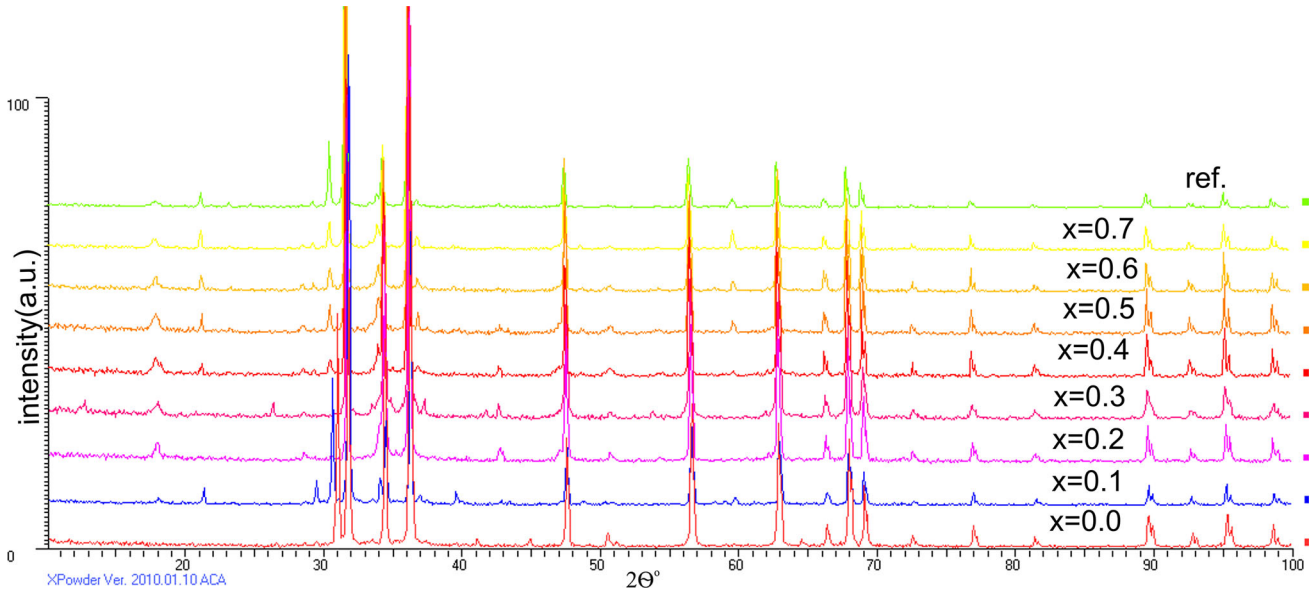

Fig. 1 Composite XRD patterns of $Zn_{1-x}Li_xO$ ($x = 0.00$ to 0.70, including reference) samples at diffraction angular range of 10° to 100° 2θ in a normalized intensity scale, showing Li solubility up to $x = 0.40$

Table 1 2θ peak positions of $Zn_{1-x}Li_xO$ samples ($x = 0.00$–0.70) and respective *hkl* values

Hkl	ZnO (2Θ°)	$Zn_{0.9}Li_{0.1}O$ (2Θ°)	$Zn_{0.8}Li_{0.2}O$ (2Θ°)	$Zn_{0.7}Li_{0.3}O$ (2Θ°)	$Zn_{0.6}Li_{0.4}O$ (2Θ°)	$Zn_{0.5}Li_{0.5}O$ (2Θ°)	$Zn_{0.4}Li_{0.6}O$ (2Θ°)	$Zn_{0.3}Li_{0.7}O$ (2Θ°)
100	31.7499	31.9919	31.8781	31.7257	31.7515	31.7118	31.8739	31.6743
002	34.4334	34.7807	34.6233	34.4571	34.5222	34.4543	34.5761	34.3843
101	36.2445	36.4953	36.3813	36.2330	36.2159	36.2159	3 6.3640	36.1679
102	47.5530	47.8369	47.7209	47.5616	47.6257	47.5568	47.6951	47.5146
110	56.5774	56.8119	56.6911	56.5547	56.5802	56.5355	56.6766	56.4920
103	62.9010	63.1530	63.0270	62.9169	62.9058	62.9248	63.0203	62.8499
200	66.3270	66.5765	66.4053	66.3035	66.2994	66.3045	66.4484	66.2349
112	67.9389	68.1701	68.0778	67.9370	67.9684	67.9202	68.0661	67.8911
201	69.0278	69.3314	69.1738	69.0663	69.0275	69.0316	69.1575	69.006
004	72.6827	72.9944	72.8461	72.7230	72.7028	72.7283	72.7236	72.6124
202	76.8724	77.1106	77.0976	76.8850	76.9475	76.8594	76.9970	76.9640
104	81.4725	81.7108	81.6665	81.5506	81.5386	81.5416	81.6087	81.6289
203	89.6769	89.8028	89.6998	89.6890	89.5746	89.5883	89.6729	89.5318
210	92.7137	92.9015	92.7985	92.6728	92.6825	92.6448	92.7651	92.7328
211	95.3080	95.4272	95.3035	95.1973	95.2215	95.1731	95.4064	95.1591
114	98.6232	98.9536	98.8820	98.6506	98.7494	98.6802	98.7512	98.5950

Concerns have been raised on phase transition which some workers [6] claimed there is no evidence for it at atmospheric pressure, rather, the existence of Li-induced structural disorder and a high-temperature phase transition. Further, dielectric, ferroelectric hysteresis loop and specific heat anomalies have been reported in Li-doped ZnO thin films and ceramics. But some workers [4] reported studies of ferroelectric properties and the effect of Li^+ and mg^{2+} dopants in ZnO bulk samples in which the ferroelectric transition temperature was reported at 330 K for $Zn_{1-x}Li_xO$, at $x = 0.15$. On the other hand, ellipsometric investigations of phase transition of $Zn_{0.8}Li_{0.2}O$ failed to confirm the ferroelectric phase transition.

In the current work, the solubility limit, structural phase transition temperatures and impedance and dielectric properties of $Zn_{1-x}Li_xO$ ($0.10 \leq x \geq 0.70$, 0.0 being

Table 2 Computed lattice constants, *c*/*a* ratio and bond length of $Zn_{1-x}Li_xO$ samples ($x = 0.00$–0.70)

Samples	*d* (Å)	Lattice constant (*a*) (Å)	Lattice constant (*c*) (Å)	*c*/*a* Ratio	Zn–O bond length (Å)
ZnO	2.60463	3.0075	5.2093	1.73210	1.8811
$Zn_{0.9}Li_{0.1}O$	2.57942	2.9784	5.1588	1.73207	1.8629
$Zn_{0.8}Li_{0.2}O$	2.59078	2.9915	5.1816	1.73211	1.8711
$Zn_{0.7}Li_{0.3}O$	2.60290	3.0055	5.2058	1.73209	1.8799
$Zn_{0.6}Li_{0.4}O$	2.59814	3.0000	5.1963	1.73210	1.8765
$Zn_{0.5}Li_{0.5}O$	2.60310	3.0058	5.2062	1.73205	1.8801
$Zn_{0.4}Li_{0.6}O$	2.59421	2.9955	5.1884	1.73206	1.8736
$Zn_{0.3}Li_{0.7}O$	2.60824	3.0117	5.2165	1.73208	1.8838

Table 3 Computed crystallite size, *D* of $Zn_{1-x}Li_xO$ crystals ($x = 0.00$–0.70) with respective *hkl* values

Hkl	ZnO (nm)	$Zn_{0.9}Li_{0.1}O$ (nm)	$Zn_{0.8}Li_{0.2}O$ (nm)	$Zn_{0.7}Li_{0.3}O$ (nm)	$Zn_{0.6}Li_{0.4}O$ (nm)	$Zn_{0.5}Li_{0.5}O$ (nm)	$Zn_{0.4}Li_{0.6}O$ (nm)	$Zn_{0.3}Li_{0.7}O$ (nm)
100	41.733	41.761	41.719	41.719	41.719	41.719	41.719	41.719
002	42.021	31.540	42.071	42.000	31.540	42.000	42.071	63.000
101	42.235	42.285	42.285	42.213	31.700	42.213	42.285	42.213
102	43.845	32.956	32.913	43.845	32.913	43.845	32.222	34.175
110	34.175	34.222	34.222	34.175	34.175	34.175	34.222	34.175
103	28.254	35.337	28.254	35.287	35.287	28.254	23.536	35.287
200	35.948	36.000	28.775	47.977	35.948	35.948	47.977	35.948
112	29.043	36.367	29.077	36.314	29.043	36.314	29.077	36.314
201	36.543	29.282	29.247	48.727	29.247	29.247	24.387	29.594
004	24.923	12.486	24.948	24.923	12.462	24.923	29.914	10.880
202	38.441	38.512	25.667	38.441	25.640	51.228	30.800	25.640
104	26.484	26.540	26.540	26.512	13.256	26.512	26.512	13.263
203	21.232	56.700	56.571	28.318	42.429	56.571	56.571	56.571
210	58.154	58.280	58.154	58.154	43.615	58.154	58.154	21.827
211	22.355	59.648	59.542	59.542	59.542	59.542	29.806	59.542
114	50.502	19.001	18.986	50.502	18.957	50.502	50.600	50.502

pristine sample) have been studied in order to elucidate some of the above problems.

2 Experimental

Analytical grade ZnO (99.99 %), Li_2CO_3 (99.99 %), ethanol (99.7 %), toluene mixed with polyvinyl chloride and distilled water were used for the preparation of $Zn_{1-x}Li_xO$ ($0.10 \leq x \geq 0.70$) by solid-state reaction. Stoichiometric amounts of the powders were thoroughly mixed and ground, and 10 ml of ethanol was added to aid homogeneity. The mixture was placed in a platinum crucible in an RHF 1600 carbolite England furnace for calcination at 1073 K for 8 h in air atmosphere. The obtained white powder was thoroughly ground using an agate mortar and pestle and further pressed into disc pellets of 19 mm in diameter and 4 mm thickness with three drops of toluene mixed with polyvinyl chloride as binder. A pressure of 137,900 kN/m^2 was used. The prepared pellets were sintered at 1473 K for 10 h in air atmosphere and furnace cooled.

Phase identification and crystalline properties of the samples were studied using X-ray diffraction (Pan Analytical, X'pert Pro) in reflection–transmission mode using Cu Kα radiation at 1.54060 Å at 30 kV and 10 mA in the 2θ range $10^{\circ} \leq 2\theta \geq 100°$ with scan time 29.85 s and scan step size of 0.064° in continuous scan mode. Using a Phenom-World scanning electron microscope (SEM) at 15 kV, the microstructure was determined at different magnifications on specimens of sintered samples. Specimens were also characterised using differential thermal analysis (DTA) (NETZSCH DTA 404 PC) in the

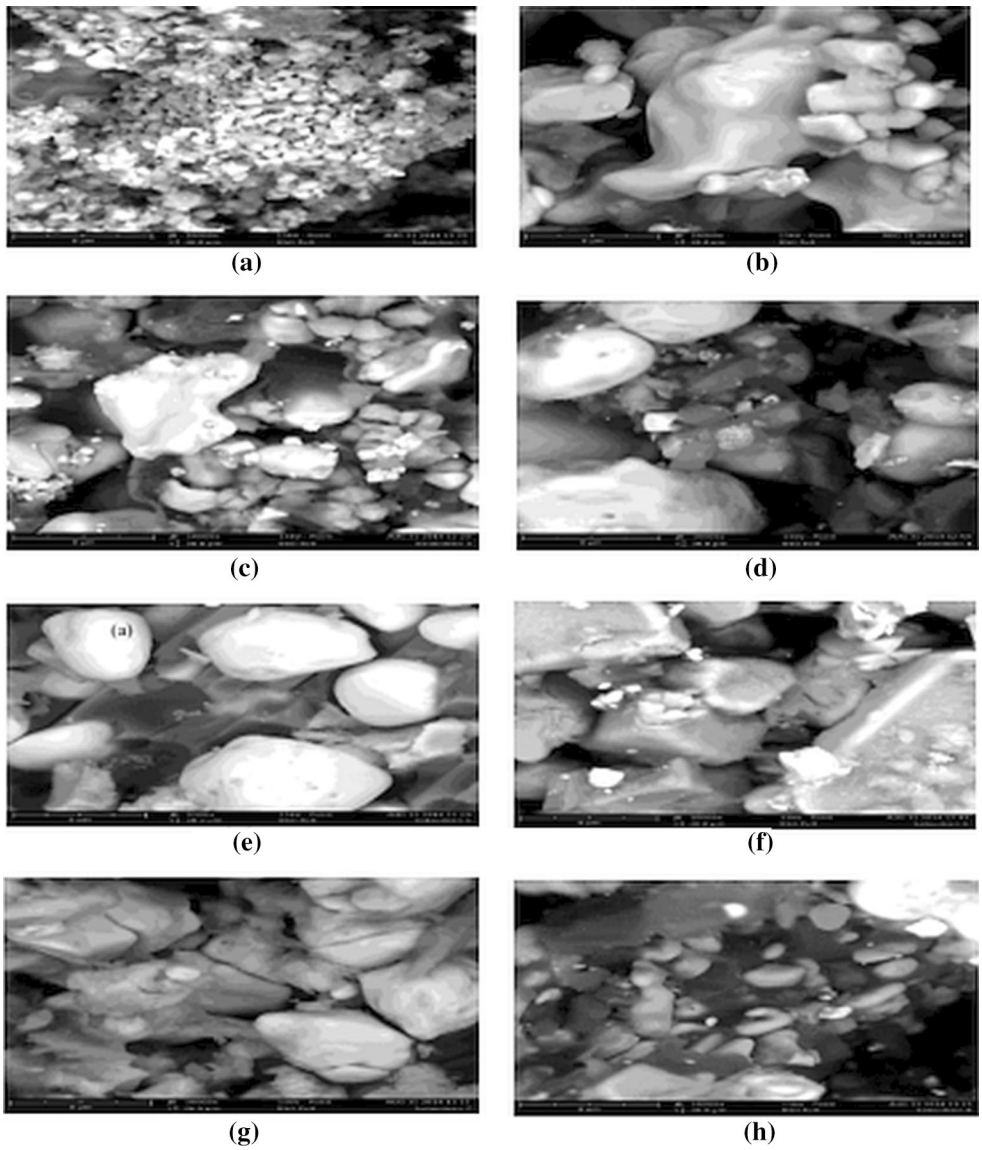

Fig. 2 SEM Images of $Zn_{1-x}Li_xO$ (x = 0.00 to 0.70) samples at magnification of $\times$10,000 showing porous regions and agglomerations, **a** undoped ZnO (x = 0.00) **b** $x = 0.10$ **c** $x = 0.20$ **d** $x = 0.30$ **e** x = 0.40 **f** x = 0.50 **g** x = 0.60 and **h** x = 0.70

temperature range 300–573 K at a heating rate of 20 K/min to determine the structural phase transformations. DTA is a thermoanalytic technique in which a material under study and an inert reference are made to undergo identical thermal cycles, while recording any temperature difference between sample and reference. The differential temperature is then plotted against time, or temperature (known as DTA curve, or thermogram). Changes in the sample could either be exothermic or endothermic and can be detected relative to the inert reference. The DTA curve thus provides data on the transformations that have occurred, such as glass transitions, crystallisation, melting and sublimation.

Impedance data were collected for eight samples for the real (Z') and imaginary (Z'') parts versus frequency f. The data were collected for all the samples at 23 °C and 46 % relative humidity. Measurements were also taken on the specimens of the samples as a function of temperature for $x = 0.0$, 0.1, 0.2 and 0.3 at temperatures 50, 100, 150 and 200 °C, each using AC fields of 50 or 10 mV and an equilibration time of 15 min. 100 nm Au sputter and Ag electrode (air-dry) paste (cured at 80 °C for 10 min) were used. Measurements were taken using an Ametek Modular impedance analyser. The geometric density of the sample was 43 % (density of ZnO = 5.606 g/cm^3).

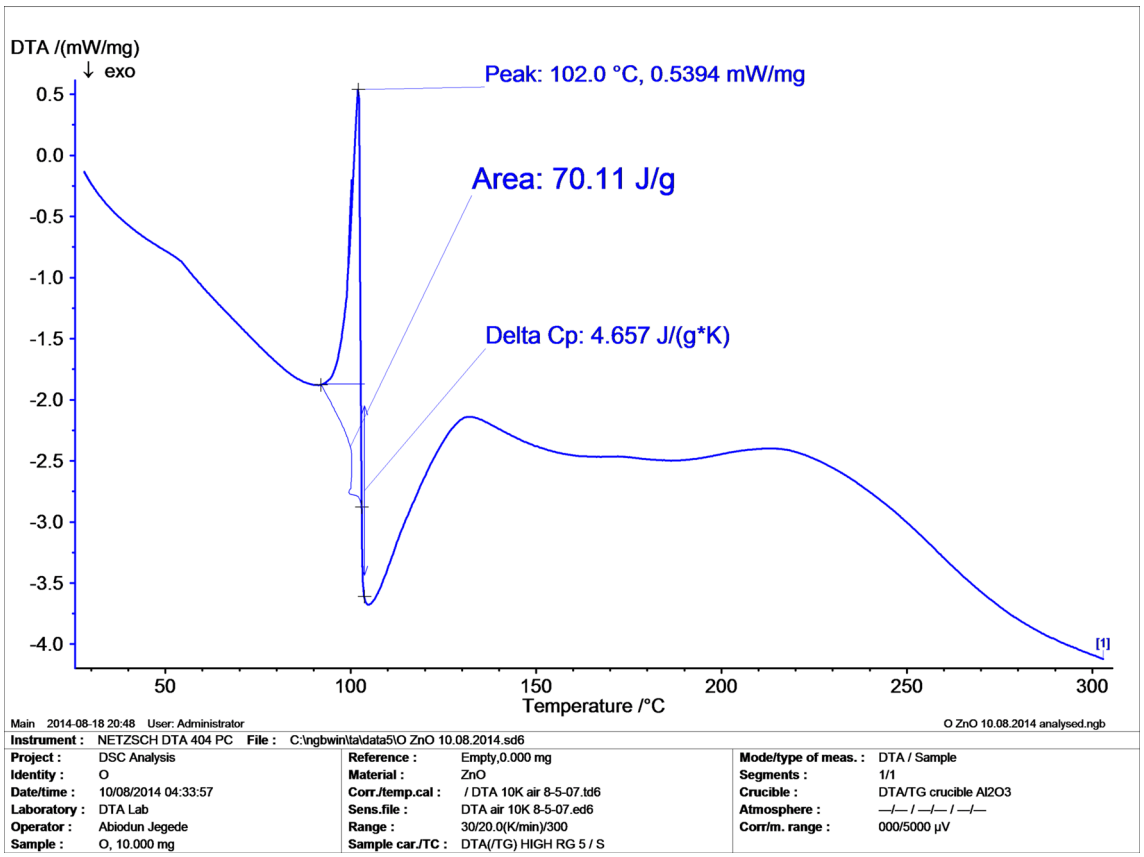

Fig. 3 Representative DTA plot of pristine ZnO ($x = 0.0$) showing the transition temperature

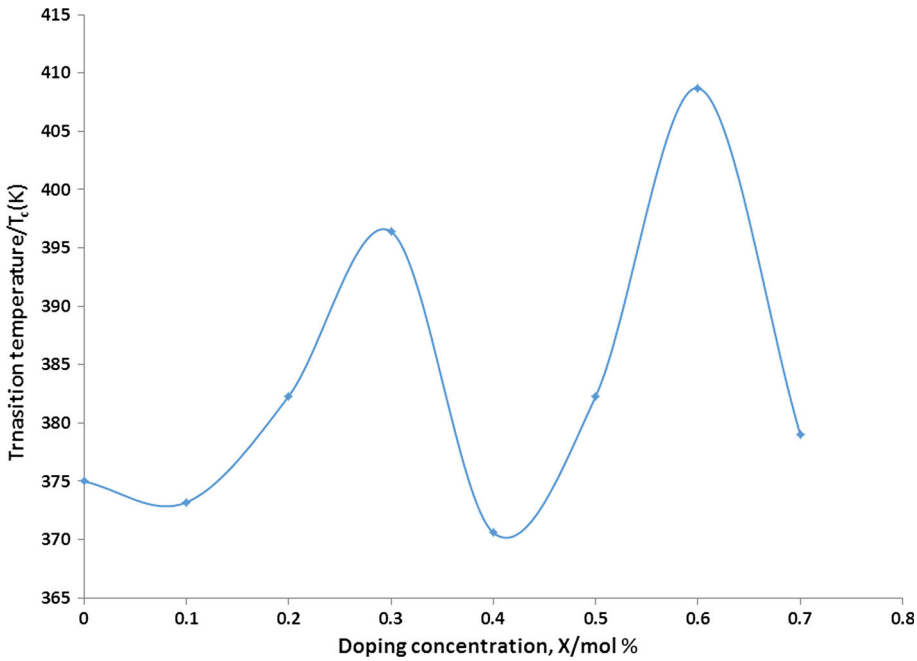

Fig. 4 Variation of transition temperatures with increase in Li concentration in ZnO ceramic

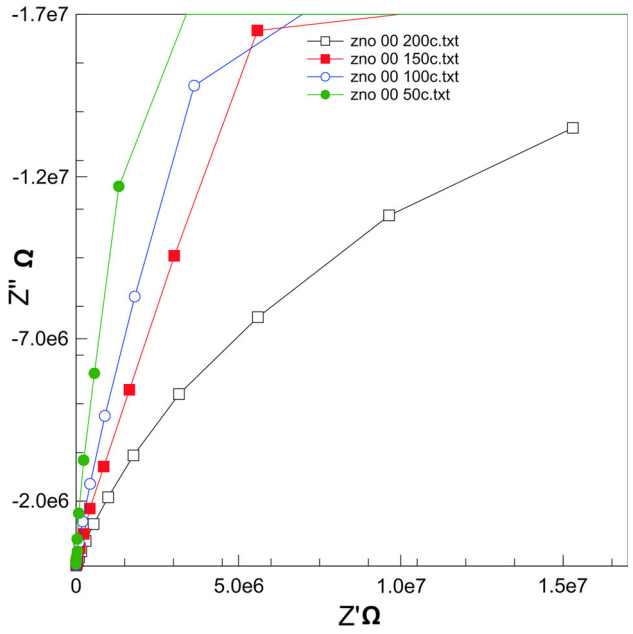

Fig. 5 Composite impedance plot of pristine ZnO ($x = 0.0$) at selected temperatures

3 Results and discussion

Figure 1 shows the result of the X-ray diffraction pattern for $x = 0.0$–0.7, including the reference pattern. It matches the reference ICSD, 1997 crystal pattern which indicates the synthesised compounds are crystalline and hexagonal in structure with minor impurity peaks as observed by other workers [6, 7]. The peaks lie between 20° and 30° ($x = 0.5$) and between 10° and 20° and at 43° 2θ, respectively, for $x = 0.60$ and 0.70. The result suggests the solubility limit of Li in ZnO is up to $x = 0.4$ and thus contrasts with that reported by other workers [8]. As the amount of lithium increased, the angle at which 2θ begins reduces indicating that more interstitial sites become occupied in agreement with earlier works [7, 9]. Slight shifts in peak positions (Table 1) to lower and higher angles as a function of doping concentration have been reported [10] and attributed to various factors such as competition between tensile and compressive stress in the lattice structure, the substitution of Zn atoms by Li atoms and to the presence of Li atoms at the interstitial sites [11]. These have been reported to lead to lattice distortion [12] and changes in ferroelectric properties [13]. Systematic shifts in peak positions to higher values with increase in Li content were not observed contrary to what has been reported [5]. The slight decrease in peak intensity is apparent in some compositions and has been attributed to the reduction in atomic mass as a result of the substitution of Li atoms (ionic radii, 0.68 Å) at the lattice sites of Zn^{2+} atoms (ionic radii, 0.74 Å) [1, 10]. Also, the relative intensity of the (101) peak is the same for all the samples at 100 % intensity and may be related to the preferred orientation [7]. The determined lattice parameters (Table 2) of the Li-doped ZnO are slightly different from those of the pristine sample and are in agreement with the result of other workers [14] who attributed it to the substitution by Li atoms which results in a slight difference in their c/a ratios. This shows that ZnO is still hexagonal though with slight distortions [7]. Reductions also occur in the Zn–O bond length and further confirm the substitution of Zn by Li. The crystallite sizes (Table 3) are virtually the same for all samples, irrespective of level of doping [7].

The result of microstructural characterisation is shown in Fig. 2a–h at a magnification of ×10,000. The undoped ZnO has a close-packed morphology with average grain size of 2.18 μm, whereas this is absent in the doped samples where agglomeration of the grains is observed in some regions in $x = 0.20$–0.60. Porous domains are also visible in all the samples and have been reported [15] to be due to the segregation of insoluble Li atoms at the grain boundaries [10]. The shape of the grains changes from hexagonal to cylindrical as the doping increased, and the average grain size for the Li-doped samples also increased in the order 1.90, 2.63, 4.35, 4.70, 5.15 and 2.40 μm, respectively, $x = 0.50$ having the largest grain size.

There are no phase transformations observed below 300 K in ZnO (doped/undoped) as shown in the representative DTA plot in Fig. 3 for $x = 0.0$. This is in accordance with reported results [12]. The plot of undoped ZnO shows anomaly which corresponds to a phase transition at a temperature of 375 K with steep and narrow peaks which are indicative of a first-order structural phase transformation. For the Li-doped ZnO, the transition temperatures increase (Fig. 4) with increase in Li doping in accordance with the result obtained by some workers [12]. This contradicts the work reported on $Li_{0.3}Zn_{0.7}O$ and pure ZnO in which they found no phase transformation from 373 to 423 K. From 408 to 377 K, there is a decrease in transition temperature for $x = 0.5$ and 0.6 with subsequent increase to 379 K in $x = 0.70$. The peaks of the DTA plots of doped ZnO samples are broader than those of the undoped ZnO. There is almost first-order phase transition in the doped ZnO which is attributed to Li atoms occupying off-centred positions where the order–disorder characteristics relating to transitional shifts of Zn and O sublattices have effect on the phase transition [12] causing dielectric anomalies. The sample with the highest transition temperature is $x = 0.6$, while the one with the highest grain size (when compared with the SEM results) is $x = 0.5$.

Impedance measurements were taken at room temperature for all the samples and at selected temperatures 50, 100, 150 and 200 °C, for $x = 0.0$–0.4.

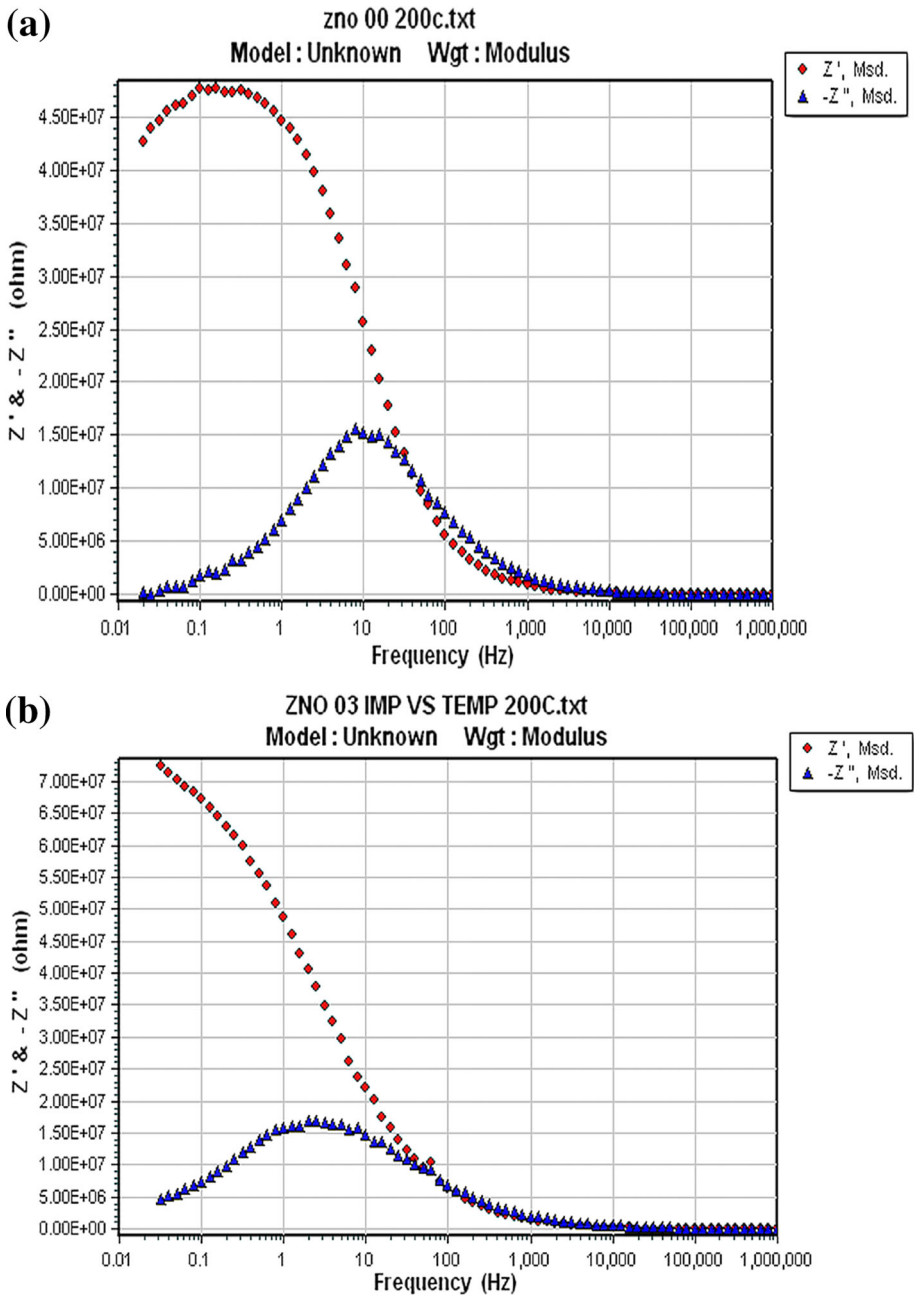

Fig. 6 Real and imaginary impedance vs frequency plot at 200 °C for representatives $x = 0.00$ (**a**) and $x = 0.3$ (**b**)

Figure 5 shows the composite impedance plot of $x = 0.0$ taken at the selected temperatures and plotted using *ZVIEW* program. It can be seen that the curvature of the impedance curves increases with increase in temperature indicating a reduction in resistance. The curve at 200 °C has the greatest curvature. Figure 6a, b is a plot of impedance (real and imaginary) versus frequency for representatives $x = 0.0$ and 0.3 at temperature of 200 °C obtained using the software *ZSim*. The square legends (in red) represent the real values of measured (Msd) impedance (Z'), while the blue triangles represent the imaginary part (Z''). The plots show relaxation behaviour and the frequencies shift from lower to higher values with increase in lithium content at the same temperature. A broad relaxation peak which indicates a distribution in relaxation times, with the difference between the peaks of the Z', Z'' versus frequency being about two decades of frequency, exhibits non-Debye character. Non-Debye behaviour is due to the absence of a single relaxation time and can be determined from the plot of z' versus $\log f$ in which the width at half height is greater than 1.14 decades of frequency and also suggests departure from ideal Debye behaviour [16].

Figure 7a–c shows representative plots of impedance for $x = 0.0$, 0.2 and 0.3 at temperature of 200 °C fitted to the

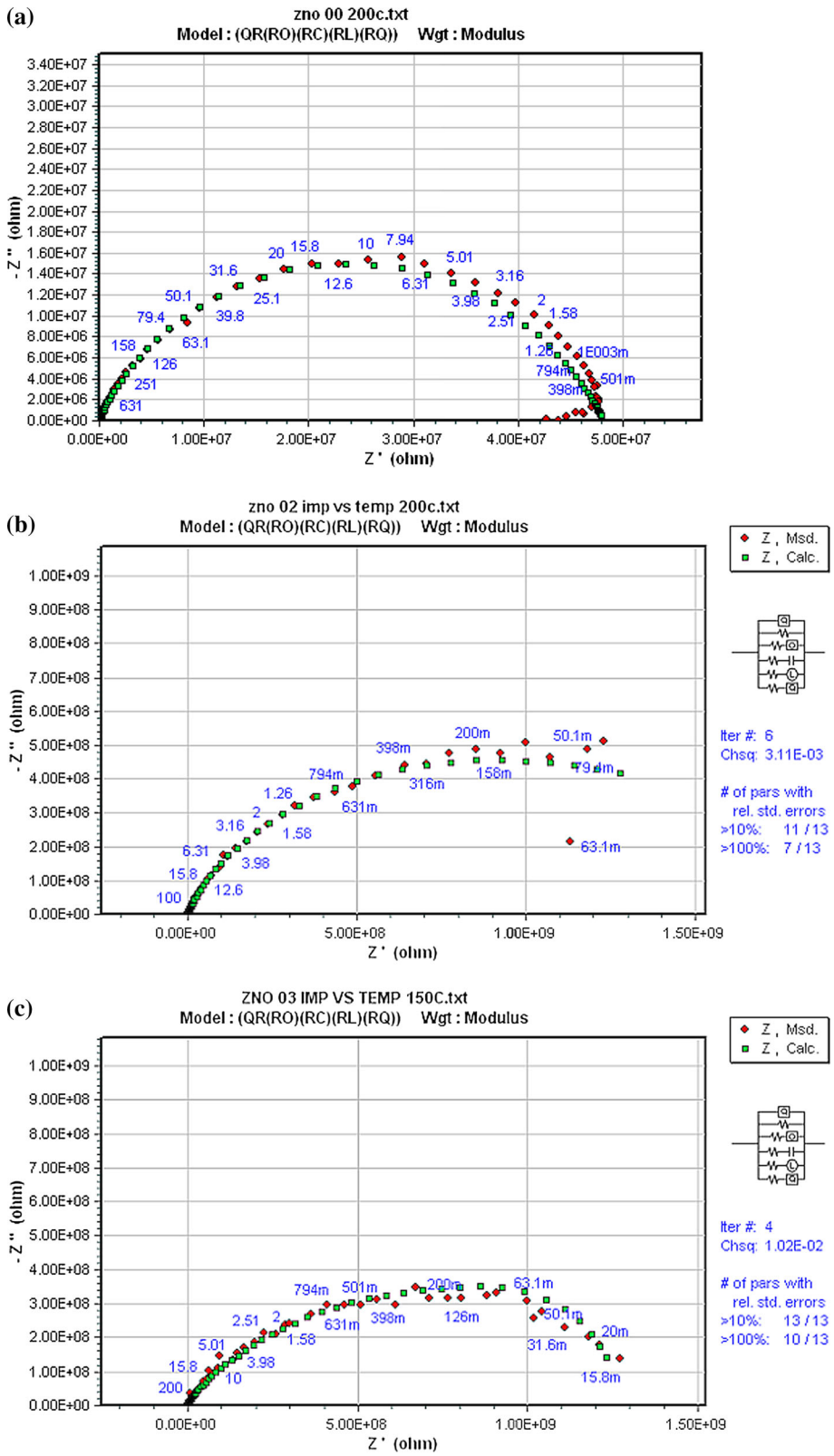

Fig. 7 Representative plots of impedance (imaginary vs real) for $x = 0.0$ (**a**), 0.2 (**b**) and 0.3 (**c**) at temperatures of 200, 200 and 150 °C, respectively fitted to the same circuit model

same circuit model. The numbers on the curves indicate the frequencies, the green squares the fit and the red squares the measured values of impedance. It is clear that the impedance curve of $x = 0.0$ (Fig. 7a) is a single semicircle similar to that of $x = 0.2$ (Fig. 7b) which though is not a complete semicircle but shows it is single arc and has lower

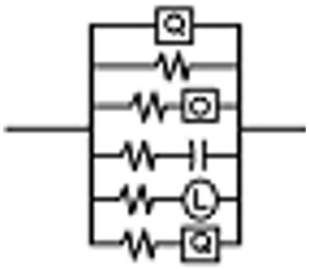

Fig. 8 The circuit model for the fitting, Q represents constant phase element, R resistance, C capacitance and L inductance

impedance value due to its higher Li content. All the samples have single arcs without separation between grain and grain boundaries (the frequency increases in an anti-clockwise direction). The single arc result has been reported [17] and references therein, where it was attributed to the conduction processes through the grain and grain boundary having the same time constants and to the fact that the model used has resistive grain boundaries and conducting grain cores [17]. The intersection of the arc with both impedance axes is at zero. The circuit model used for the fitting is shown in Fig. 8, where Q represents constant phase element, R resistance, C capacitance and L inductance. Four iterations were used to obtain the fit with Chi-square value of 1.23×10^{-3} (Fig. 7a). Thirteen parameters were used for the fitting (which is not perfect) with ten having relative standard error greater than 10 %. In Fig. 7b, the number of iterations is six and the same thirteen parameters (eleven have relative standard error greater than 10 %) were needed for the fit, the Chi-square values being 3.11×10^{-3}. Figure 7c shows a similar plot fitted to the same circuit model described above but at lower temperature of 150 °C ($x = 0.2$) in which only four iterations were used and the Chi-square value is much smaller at 1.02×10^{-2}. Visual inspection shows an almost perfect fit, but fitting parameters indicate there are still some mismatches.

Figure 9 is a composite plot of the permittivity (dielectric constant) plotted at different frequencies for all the samples at room temperature. The patterns show the characteristic dispersion of dielectric constant with increase in frequency. The dielectric constant falls with increase in frequency and decreases much faster for $x = 0.0$, 0.3, 0.4 and 0.7, becoming almost independent of temperature at high frequencies, particularly for $x = 0.2$ which has a value of ~ 7. Polarisation in dielectrics has been attributed to many factors, such as space charge effects, dipole orientation, electronic. The high values of the dielectric constant at low frequencies could be attributed to space charge effects resulting from charge accumulation because of DC conductivity. However, at high frequencies, interfacial polarisation increases hence the saturation or constant value of dielectric constant. Also, the dipoles can no longer follow the field fast enough and therefore tend towards static values at all temperatures [16]. A maximum value of dielectric constant has been reported [8] for all frequencies at the same concentration of $x = 0.2$, on the contrary, and has been attributed to lattice mismatch between Zn and Li ions. Further work is required to explain this behaviour. Also, around 150 Hz, small wiggles in the dielectric constant are clearly seen in all the

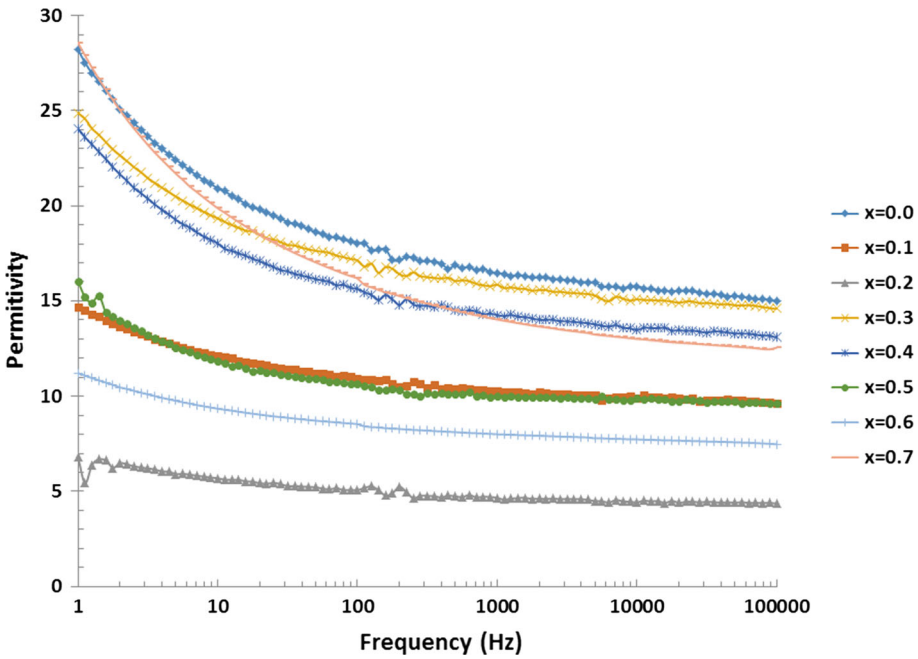

Fig. 9 Composite plot of the permittivity (dielectric constant) vs frequency plotted at different frequencies for all the samples at room temperature

samples at room temperature and may be related to structural transformation that may have occurred. Some workers [14] have reported dielectric anomaly at 330 K for Li-doped ZnO at $x > 0.1$ [8], and a similar report of a dielectric phase transition has been found between the ferroelectric and paraelectric phase at 330 K for Li-doped system for $x = 0.15$ [4]. Since the temperature is in the vicinity of room temperature, it could be responsible for the behaviour. Similarly, other workers have reported small peaks around 15–35 °C in the dielectric constant in Li-doped samples measured in air atmosphere [15]. Further work such as DC electrical conductivity and Raman spectroscopy studies carried out at this frequency may be helpful. There is generally an increase in dielectric constant with increase in Li content with the highest dielectric constant obtained for $x = 0.0$ and 0.7 being $\sim$28.0. The value of dielectric constant for pristine $x = 0.0$ reported to be $\sim$9 [5] is high and could be due to the presence of water vapour in the atmosphere [15] which has been found to increase the dielectric constant at room temperature, given the relative humidity reported at the experimental condition.

4 Conclusion

ZnO was prepared by solid-state reaction, and phase analyses of the samples show that they are polycrystalline and majorly of single phase with hexagonal structure. The lattice parameters were found to reduce (a, c) with the c/a ratio almost constant for all samples, which is an indication that the crystal structure did not change but suffers some slight distortion. The crystallite size appears to be independent of doping level with solubility limit at $x = 0.4$, but the grain size increased with increase in Li content. Agglomeration was observed in some of the samples' microstructure. Phase transition analyses show that all Li-doped samples have no phase change near room temperature and the transition temperatures generally increase up to a maximum with increase in Li doping before decreasing at certain levels of Li doping. At 375 K, a phase transformation was observed for undoped ZnO which increased as Li concentration increased with the highest temperature being $\sim$409 K for $x = 0.6$. Impedance results show a general increase in dielectric constant with increase in Li doping, while the impedance curves are characterised by single arcs which show relaxation behaviour that is non-Debye. Further work is required in order to resolve issues like the dielectric anomaly at $\sim$150 Hz and the very low dielectric constant of $x = 0.2$. This implies that Li-doped ZnO still has some peculiarities.

References

1. V. Bilgin, J. Electron. Mater. **88**, 1969–1978 (2009)
2. A.H. Salama, J. Mater. Sci. Technol. **25**, 314–315 (2009)
3. A. Janotti, Van de Walle, Rep. Progr. Phys. **72**, 126501 (2009)
4. D.S. Singh, J. Nagaraju, S.B. Krupanidhi, J. Appl. Phys. A **88**, 421–424 (2007)
5. S.H. Jeong, B.N. Park, S.-B. Lee, J.-H. Boo, J. Thin Solid Films **516**, 5586–5589 (2007)
6. Y.L. Du, Y. Dengi, M.S. Zhang, Solid State Commun. J. **137**, 78–81 (2005)
7. M.K.R. Khan, M.M. Rahman, I. Tanaka, Nucleus **39**, 149–154 (2003)
8. M.K.R. Khan, M. Rahman, S.J. Mia, M. Shahajahan, Indian J. Pure Appl. Phys. **41**, 211–216 (2003)
9. S. Polarz, A. Orlov, A. Hoffmann, M.R. Wagner, C. Rauch, R. Kirste, M. Lehmann, Chem. Matter **21**, 3889–3897 (2009)
10. M. Ardyanian, N. Sedigh, Bull. Mater. Sci. **37**, 1309–1314 (2014)
11. Y. Zeng, Z.Z. Ye, W.Z. Xu, L.I. Chen, D.Y. Li, L.P. Zhu, Y.L. Hu, J. Cryst. Growth **283**(1), 180 (2005)
12. X.S. Wang, Z.C. Wu, J.F. Webb, Z.G. Liu, Appl. Phys. A **77**, 561–565 (2003)
13. J.S. Kim, H.J. Lee, H.J. Seog, W. Kim, J. Korean Phys. Soc. **58**, 640–644 (2011)
14. A. Onodera, N. Tamaki, K. Jin, H. Yamashita, Jpn. J. Appl. Phys. **36**, 6008 (1997)
15. A. Sokiassian, A. Tganstsev, N. Seller, Appl. Phys. Lett. **07**, 192903 (2010)
16. U. Ahmadu, T. Salkus, A.O. Musa, K.U. Isah, Open J. Phys. Chem. **1**, 94–103 (2011)
17. Z. Zhou, K. Kato, T. Tomaki, M. Yoshino, H. Yukawa, M. Morinaga, K. Morita, J. Eur. Ceram. Soc. **24**, 139–146 (2004)